

Angle-resolved de Haas–van Alphen study of SrRuO₃

C. S. Alexander,* S. McCall,[†] P. Schlottmann, and J. E. Crow[‡]

National High Magnetic Field Laboratory, Florida State University, Tallahassee, Florida 32310, USA

G. Cao

Department of Physics and Astronomy, University of Kentucky, Lexington, Kentucky 40506, USA

(Received 16 July 2004; revised manuscript received 9 February 2005; published 7 July 2005)

The results of angle-resolved de Haas–van Alphen oscillations in SrRuO₃ single crystals are reported. At least six fundamental frequencies of oscillation are detected between 100 and 11 000 T. The effective mass of the charge carriers is measured for each orbit and ranges from 4.1 to 6.9 m_e . The mean free path length of the charge carriers is between 640 and 5500 Å or roughly 100–1000 times the unit cell dimensions. The measured frequencies are compared to the Fermi surface calculated by Santi and Jarlborg.

DOI: [10.1103/PhysRevB.72.024415](https://doi.org/10.1103/PhysRevB.72.024415)

PACS number(s): 74.70.Pq, 71.18.+y, 71.20.Be

I. INTRODUCTION

Even though it has been studied for over 40 years,¹ a thorough understanding of the electronic structure of the itinerant ferromagnetic metal SrRuO₃ remains elusive. SrRuO₃ is a member of the layered strontium-ruthenate Ruddlesden-Popper series. Single layer Sr₂RuO₄ is a superconductor possibly with p -wave spin-triplet pairing.² Bilayer Sr₃Ru₂O₇ shows no evidence for magnetic long-range order, but does possess two metamagnetic transitions and a magnetic field tuned quantum critical point.³ The infinite layer, pseudocubic, SrRuO₃ exhibits a ferromagnetic transition at 165 K.⁴ While insight into these materials has grown over the years, there is a lack of connection between theoretical predictions of the electronic band structure and experimental results.

Numerous band structure calculations for SrRuO₃ based on the local spin density approximation (LSDA) have been reported.^{5–8} The $4d$ orbitals of ruthenium lead to strongly correlated narrow bands close to the Fermi level. In a paramagnetic band structure, the Fermi surface (FS) is determined by the number of electrons (Luttinger's theorem), while for a compound with a ferromagnetic ground state, such as SrRuO₃, the splitting of the majority and minority spin bands changes with the magnetic moment. The position of the Fermi level with respect to the band features is then less well determined. In addition, distortions of the perovskite structure also contribute to the energy balance leading to magnetic long range order. Mazin and Singh^{5,6} correctly predict ferromagnetism with an ordered Ru magnetic moment of 1.59 μ_B , in good agreement with the experimental value of 1.6 μ_B measured on films through point-contact Andreev reflection.⁹ They also obtain a strong hybridization of the Ru $4d$ electrons with the O $2p$ orbitals and significant spin differentiation in the transport properties based on the Fermi velocities. Allen *et al.*⁷ also calculated the electronic structure of SrRuO₃ and investigated its consequences on the thermodynamic and transport properties. A thorough study of the FS of CaRuO₃ and SrRuO₃ was presented by Santi and Jarlborg.⁸

Numerous agreements between theory and experiment have led to a widespread acceptance of the band structure results. However, a much stronger test is a direct comparison

of the predicted and experimentally determined FS. The FS of SrRuO₃ was previously probed through the measurement of Shubnikov–de Haas (S–dH) oscillations in the electrical resistivity of thin film samples.¹⁰ A comparison of the results of this study to the theoretical predictions is only a partial success. While some of the observed orbits fit well into the existing theories, there are other predicted orbits that are conspicuously absent. However, it is possible that these missing orbits could be accounted for by considering the restricted range of spatial orientation possible for thin film samples. This geometrical limitation (which prevented the probe of the entire FS) can be avoided by using three-dimensional single crystal samples in lieu of thin films.

The motivation of this paper is to carry out angle-resolved S–dH and de Haas–van Alphen (dH–vA) measurements in very high magnetic fields on single crystals of SrRuO₃ and compare these with the existing FS from LSDA calculations. Large magnetic fields suppress part of the strong interactions between the electrons and reduce the effective masses. Under these circumstances LSDA calculations (although they do not include all the correlations) can give accurate descriptions of the FS. LSDA calculations have been used with a high rate of success in predicting the band structure of many systems including some very highly correlated electron systems such as UPt₃¹¹ and the superconductor Sr₂RuO₄.¹²

The remainder of the paper is organized as follows. Section II is devoted to the sample preparation and characterization. In Sec. III, we briefly review the Lifshitz–Kosevich equation for the oscillations of the magnetization as a function of field and the corrections necessary to account for the demagnetization field in a ferromagnet. In Sec. IV we present and discuss the results of our angle-resolved measurements. A summary of the results and conclusions are given in Sec. V.

II. SAMPLE PREPARATION AND CHARACTERIZATION

Single crystal samples were grown using a self-flux method. Off-stoichiometric mixtures of RuO₂, SrCO₃, and SrCl₂ were placed in platinum crucibles and heated to 1500 °C. The mixture was soaked for 24 h at 1500 °C and

then cooled at 2 °C/h to 1350 °C. The samples were then rapidly cooled to room temperature in an attempt to prevent twinning. The resulting crystals were rectangular parallelepipeds with varied sizes up to $\approx 1.0 \times 1.0 \times 0.5$ mm with the short dimension always being along the *c*-axis.

Despite the rapid quench to room temperature, a sizable fraction of the crystals exhibited a twinned structure in the *ab*-plane. For this reason, and to ensure composition and phase integrity, it was necessary to carefully screen the samples used in this study. The samples were characterized with x-ray diffraction (XRD), energy dispersive x-ray analysis (EDX), differential interference contrast optical polarized light microscopy (DIC), and tunneling electron microscopy (TEM). XRD and EDX results indicated that the samples were of the SrRuO₃ phase without any measurable impurity phases. DIC data were used to find crystals untwinned down to the optical resolution of ≈ 1 μm. Twinned crystals were easily identified using this approach as the twinned regions were typically on the order of 10–100 μm in agreement with the difference in the *a*- and *b*-axis unit cell dimensions. This was later verified via TEM to much higher resolution (of the order 1 nm). Portions of the samples were studied via TEM, a destructive measurement, which also confirmed that the samples were single phased.

Following the aforementioned selection process, the samples were carefully characterized in terms of their electrical and magnetic properties to ensure that they were of the highest quality possible. The magnetic susceptibility of the samples was measured as a secondary check of the sample purity and single phased nature. It is known that doping of other elements into SrRuO₃ results in a reduction in the Curie temperature.^{4,13} For the samples used in this study T_c was determined to be 165 K, supporting the previous conclusion that they contain no significant impurity doping. Furthermore, no other magnetic phases were observed.

Electrical resistivity results indicated residual resistivity of 2 μΩ cm at 4 K and a residual resistivity ratio [$RRR = R(300\text{ K})/R(4\text{ K})$] of 140. This represents a significant improvement over previously reported data on single crystals⁴ as well as thin film samples.¹⁴ This is important in quantum oscillation experiments as the purity of the sample directly relates to the mean free path (mfp) of charge carriers. For oscillations to be observed, the mfp must exceed the length of the closed orbit.

It should be noted that there were multiple crystallites (accounting for roughly 5% of the total sample mass) attached to the primary crystal. These crystallites are not expected to influence the dH–vA or S–dH results due to the relatively small quantity and the fact that they are not evident in the XRD and magnetization data.

III. LIFSHITZ–KOSEVICH EQUATION

Oscillations in physical properties depend on the closed orbits of the FS and arise from the quantized cyclotron motion of the electrons in magnetic fields.¹⁵ According to the Lifshitz–Kosevich equations, the oscillatory part of the magnetization, M_{osc} , due to an orbit of extremal area A_e perpendicular to the applied field \mathbf{B} is given by

$$M_{\text{osc}} \propto (m_{\text{perp}} B)^{1/2} R \sin\left(s \frac{2\pi f}{B} + \gamma\right), \quad (1)$$

where the frequency of oscillation, $f(\mathbf{B}) = (\hbar/2\pi e) A_e(\mathbf{B})$, is proportional to the area of the extremal orbit and thus dependent on the orientation of the sample in the applied field. Here s denotes the order of the harmonic, γ is a phase, and m_{perp} is the effective mass perpendicular to the orbit. R is a damping factor accounting for decreased oscillation amplitude due to the smearing of the FS orbit by temperature and scattering. The effective mass, m^* , of the charge carriers can be determined through $R = X/\sinh X$, where $X = 2\pi^2 s k_B (T + T_D) m^* / (\hbar e B)$ and T_D is the Dingle temperature, which is a parameter related to the lifetime of the quasiparticles and represents scattering of the carriers out of the closed orbit.

B represents the magnetic field experienced by the charge carriers. In a paramagnetic metal this is simply the external magnetic field. In the case of a ferromagnetic metal, however, the demagnetization field internal to the sample reduces the applied field. For a saturated ferromagnet, the demagnetization field is given by $4\pi D M$, where M is the magnetization and D is the demagnetization factor, a geometric factor that depends on the sample geometry and its orientation in the field. Low field magnetization measurements taken in a dc SQUID magnetometer were used to determine the demagnetization factor for each sample. The saturation magnetization was measured with a vibrating sample magnetometer in applied fields up to 30 T. These data were combined and used to determine the demagnetization field present in the samples.

Due to magnetic breakdown,¹⁶ oscillations corresponding to frequencies that are linear combinations of extremal FS cross sections may occur in the presence of large magnetic fields. In addition, frequency mixing may also occur as a consequence of ferromagnetic long range order.¹⁷ The electrons experience the magnetic induction rather than the applied field and the magnetic induction contains the dH–vA oscillations. The resulting nonlinear equation again yields frequencies that are linear combinations of extremal FS cross sections. This phenomenon has been observed in various metals.¹⁸

IV. RESULTS AND DISCUSSION

The magnetoresistance (MR) was measured at 30 mK in order to provide an independent verification for subsequent dH–vA measurements as well as to establish a connection with previous experiments.¹⁰ The data were collected using a standard four-probe technique with the electrical contacts placed linearly in the *ab*-plane along either the *a*- or *b*-axis. Low current ac techniques were used due to limitations on the heat load that would be dissipated in the sample at the temperatures of interest. The magnitude of the resistivity was calibrated using dc techniques at higher temperatures where heat dissipation is not an issue.

Resistivity data with applied magnetic field in the *ab*-plane are shown in Fig. 1(a). S–dH oscillations are barely perceptible in the raw data due to the small amplitude of oscillation. However, when the smooth background MR, de-

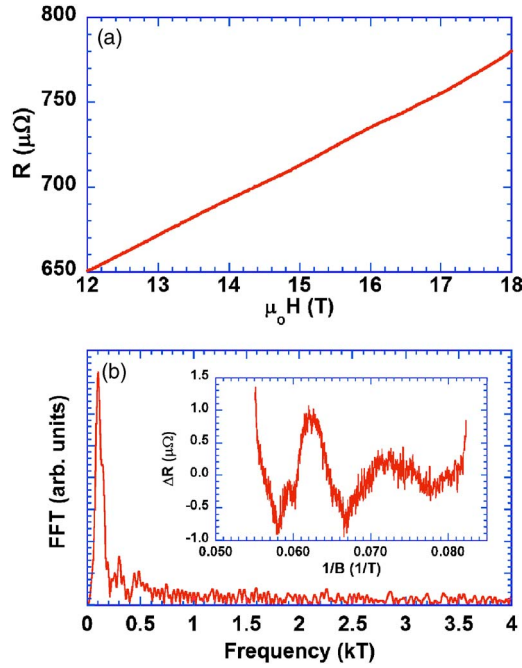


FIG. 1. (Color online). (a) Magnetoresistance data collected at 30 mK with current and magnetic field applied in the *ab*-plane; (b) frequency spectrum of the Shubnikov–de Haas oscillations present in the magnetoresistance. The inset shows the oscillations after subtraction of the background resistance.

terminated using a low order polynomial fit to the raw data, is subtracted, the oscillations become obvious as shown in the inset of Fig. 1(b). A subsequent fast Fourier transform (FFT) of the oscillation data results in the spectrum shown in Fig. 1(b), indicating a primary frequency of 100 T, which, as will be shown below, is consistent with the oscillations in the magnetization. The data also suggest the presence of higher frequency components but at much lower amplitude. These were not fully investigated in the MR, since they are better observed in the magnetization. For the same reason, no angular dependence of the field orientation was studied in the S–dH oscillations.

In a previous S–dH study,¹⁰ carried out on a high-quality thin film, two frequencies corresponding to 1.5 and 3.5 kT were identified. These frequencies (especially the 3.5 kT one) do not agree with those observed here (S–dH and dH–vA). However, it is known from band-structure calculations⁸ that the Fermi surface, especially the one of the majority spins, is very sensitive to small changes of the chemical potential, i.e., the magnetization. In a thin film the lattice can relax and the magnetization can be different due to the geometry. This could give rise to very different frequencies than for the bulk. A strong indication that this is indeed the case is that the Curie temperature for the thin films is ~ 150 K, nearly 15 K lower than that for the bulk crystals. The discrepancy could also arise from film strains unavoidably exerted by the substrate. Note that the experimental values for the saturation magnetic moment vary between 0.8 and 1.6 μ_B (see Ref. 8 and references therein) and are in general smaller than the theoretical estimates, which also vary considerably. The differences may be attributed to

finite-temperature effects, the multidomain structure and the magnetocrystalline anisotropy.

The magnetization was measured with a phosphor bronze cantilever magnetometer. Cantilever magnetometers measure the torque produced by the sample when placed in a magnetic field. This type of magnetometer is extremely sensitive to changes in magnetization but is not reliable in measuring the absolute value of the magnetization. For this reason, the results are presented in arbitrary units. Since dH–vA oscillations are not dependent on the magnitude of the magnetization, this is not a limitation to this study. The sample and cantilever system was placed in a top loading dilution refrigerator inside an 18 T-superconducting magnet at the facilities of the National High Magnetic Field Laboratory in Tallahassee, FL. The cantilever was rotated in the applied magnetic field to achieve various orientations of the applied field relative to the crystallographic axes.

For a ferromagnetic sample in an applied magnetic field, the internal magnetic field, which acts to reduce the total field, must be considered. The demagnetization factor, D , was experimentally determined from the initial slope of the magnetic susceptibility at low field. For the sample used in this study, the demagnetization factor varied from 0.78 for field applied along the *c*-axis to 0.54 for field applied in the *ab*-plane. The internal field, H_{int} , is then calculated from

$$H_{\text{int}} = H_{\text{appl}} - D 4\pi M, \quad (2)$$

where M is the magnetization measured on this sample to an applied field, H_{appl} , of 30 T. Using this method, the effective field reduction for an applied field of 15 T applied parallel to the *c*-axis ($\theta=90^\circ$) is ~ 0.15 T or 1% of the applied field. Since dH–vA oscillations are observed at high magnetic fields where the demagnetization effect is rather small, the internal field correction is almost negligible in this study.

The magnetization was measured at 30 mK for sample orientations with the applied field in the *ac*- or *bc*-plane. We did not observe significant differences in the results for the field applied in the *ac*-plane vs the *bc*-plane. This is not too surprising in view of the similarities of the theoretical Fermi surface along these directions and the slight difference between the *a*- and *b*-axis lattice parameters. Despite this it is still important to use untwinned crystals to minimize the strain in the sample and thereby reduce scattering. Field orientation is described in terms of degrees away from the *ab*-plane such that 0° corresponds to an applied field along the *a*- or *b*-axis and 90° corresponds to applied field along the *c*-axis. Data were generally collected every five degrees between these extremes, however, poor signal to noise issues resulting from geometric effects on the cantilever made measurement difficult at angles less than 20° .

Typical data for $\theta=70^\circ$ are shown in Fig. 2(a), where dH–vA oscillations can clearly be seen. Multiple frequencies of oscillation manifest as beats in the oscillation amplitude. The oscillation frequencies were determined via a similar analysis as for the magnetoresistance, i.e., the background magnetization was first subtracted and the results subsequently processed with a FFT routine. The obtained frequency spectrum for $\theta=70^\circ$ is shown in Fig. 2(b). The peaks correspond to the fundamental frequencies (identified with

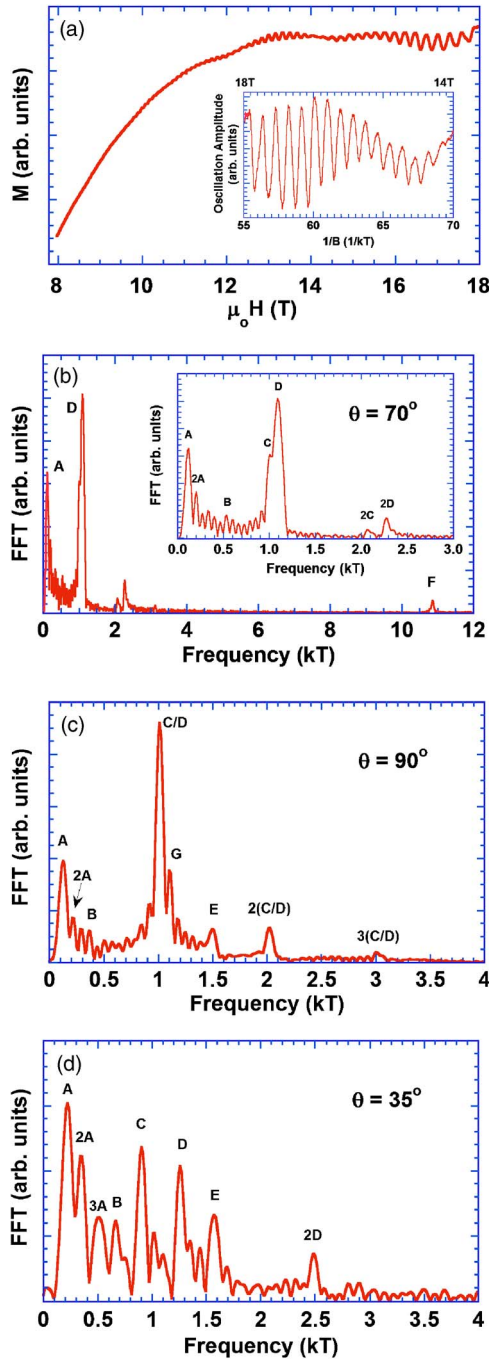


FIG. 2. (Color online). (a) Magnetization data collected at 30 mK. The applied magnetic field was 70° out of the ab -plane. The inset shows the de Haas-van Alphen oscillations present after subtraction of the background magnetization; (b) frequency spectrum of the de Haas-van Alphen oscillations for $\theta=70^\circ$. The inset shows a more detailed view of the low frequency end of the spectrum; (c) and (d) shows the frequency spectrum at 30 mK for the field parallel to the c -axis and $\theta=35^\circ$, respectively.

letters) and their harmonics. In Figs. 2(c) and 2(d) we present the FFT results for $\theta=90^\circ$ and $\theta=35^\circ$, respectively. In order to properly identify the fundamental frequencies and their harmonics it is necessary to follow their angular dependence.

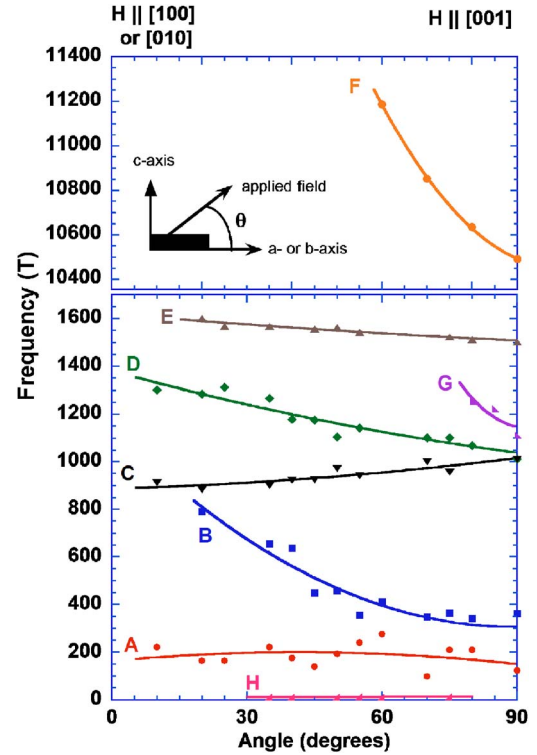


FIG. 3. (Color online). Frequency of the de Haas-van Alphen oscillations at 30 mK as a function of angle between the applied field and the ab -plane of the sample. The solid lines are a guide to the eye.

Several fundamental frequencies of oscillation are observable in the data. The dependence of the frequencies on the angle between the ab -plane of the sample and the applied field is shown in Fig. 3. Six fundamental frequencies, designated A–F, are clearly distinguished. They spread over a wide range of frequencies from 100 to 11 000 T. In addition to the fundamental frequencies, harmonics of frequencies A, C, and D are observed.

Two additional frequencies, designated G and H, are noted in the figure but remain questionable. Frequency G occurs over a very limited range of angles and is similar to other fundamental frequencies (C and D), and, hence, it may actually be a continuation of one of those frequencies. Frequency H varies between 12 and 15 T and requires a very large range of magnetic fields to observe multiple periods of oscillation. The field range used here was insufficient for a definitive determination of this frequency.

For the frequencies A–F the effective mass of the charge carriers was determined from the temperature dependence of the oscillation amplitude. This is accomplished by plotting the logarithm of the amplitude R over T [see Eq. (1)] versus the temperature. The slope in the linear dependence between $\ln(R/T)$ and T yields the effective mass of the orbit. The effective masses are in the range of 4.1–6.9 free electron masses and are listed in Table I for the field parallel to the c -axis. These values compare reasonably well with the average theoretical value of $3.7 m_e$ for the effective thermal mass predicted by Allen *et al.*⁷ Note, however, that large magnetic fields quench the mass renormalization, such that the experi-

TABLE I. Measured Fermi surface parameters for SrRuO₃.

Orbit	$f(T)$	$m^* (m_e)$	A_e (10 ¹⁴ cm ⁻²)	% First BZ	$\langle k_F \rangle$ (10 ⁶ cm ⁻¹)	v_F (10 ⁶ cm/s)	T_D (K)	τ (ps)	mfp (Å)
A	118	5.1	1.13	0.88	5.99	1.36	0.54	4.48	610
B	364	6.0	3.47	2.71	10.51	2.04	0.15	15.70	3210
C	1015	5.5	9.68	7.56	17.55	3.69	0.48	5.10	1882
D	1015	5.5	9.68	7.56	17.55	3.69	0.95	2.56	946
E	1500	6.9	14.31	11.17	21.34	3.58	1.37	1.78	637
F	10486	4.1	100.01	78.08	56.42	15.75	1.69	1.44	2265
G	1110	4.1	10.59	8.26	18.36	5.15	0.24	10.31	5306
H	13		0.12	0.10	1.99				

mental values should be below the theoretical predictions. In Fig. 4 we show the $\ln(R/T)$ vs T plots for three orbits, A, B, and G, in a field of 14 T applied parallel to the c -axis. The scattering of the data is probably due to the weak oscillating signal. The Dingle temperature is obtained for each orbit

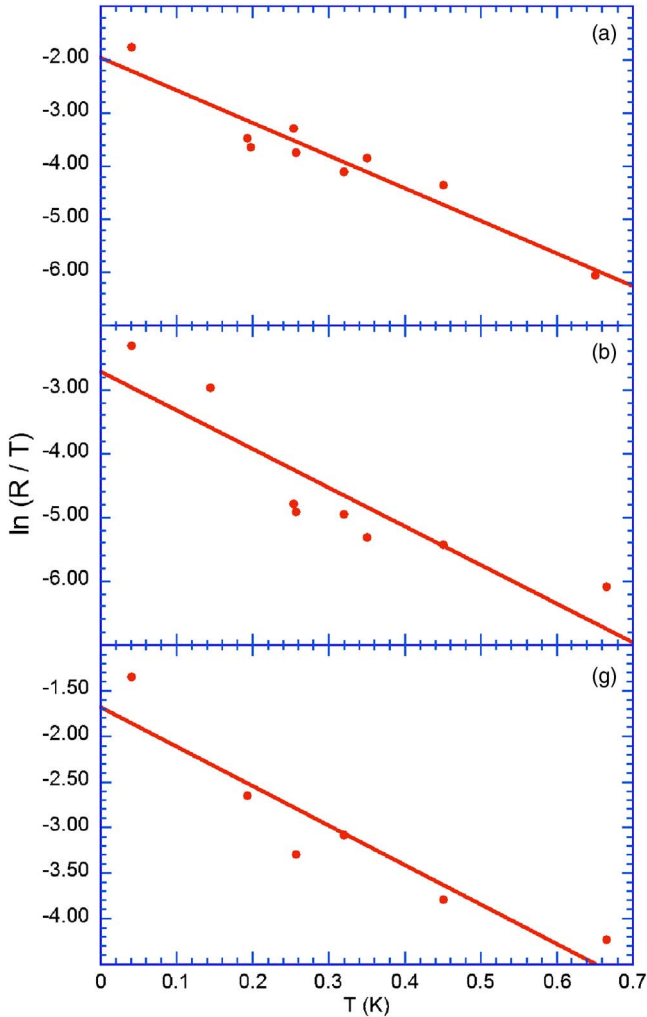


FIG. 4. (Color online). Logarithm of the amplitude over T , $\ln(R/T)$, vs T for three frequencies, A, B, and G. The slope yields the effective mass. The scatter of the data is due to the weak oscillating signal.

from the slope of a plot of $\ln(RB)$ vs $1/B$ at a constant temperature of 30 mK. Due to the scattering of the data, the uncertainty in the effective masses is $\approx 0.1m_e$ on all the orbits and the uncertainty in the Dingle temperature is roughly 0.03 K.

Also shown in Table I are the frequencies of oscillation for each orbit, measured at 90° ($\mathbf{B} \parallel [001]$). From these values the area of the orbits, the average Fermi vector and the Fermi velocities were calculated and are listed in Table I. The orbits range from only 1% to 80% of the cross sectional area of the first Brillouin zone. The average time between scattering events, τ , was calculated from the Dingle temperature and when combined with the Fermi velocity gives the mean free path of the charge carriers. These results are also summarized in Table I.

Finally, we attempt a comparison with the LSDA band structure calculations of Santi and Jarlborg.⁸ These authors calculated the sheets of the FS of SrRuO₃ for (a) the idealized simple cubic perovskite structure and (b) the real orthorhombic structure. These calculations yield totally different Fermi surfaces, confirming that the FS strongly depends on the exact structure and on the magnetization of the system. Since small changes in the polarization or the positions of the ions can produce dramatic effects on the FS, an absolute agreement with the experiment cannot be expected. Considering here Fig. 5 of Ref. 8, we observe that sheets (a) and (b) correspond to the majority spin and sheets (c)–(f) to the minority spin FS. The majority spin FS appears to be less stable to changes in the bands than the minority spin FS.

The largest frequency observed, labeled F, could arise either (i) from the “pancakes” in Figs. 5(e) and 5(f) of Ref. 8 or (ii) from the large orbit centered at the Γ -point shown in Fig. 5(e). The corresponding area in all cases is of the order of 70%–80% of the cross section of the Brillouin zone, in agreement with the experimental observation. Since the amplitude is proportional to $(m_{\text{perp}})^{1/2}$, case (ii), the orbit centered at the Γ -point, is more likely, since it has the larger perpendicular mass (along the z -direction in Ref. 8). In addition, the angular variation of the orbit would lead to an increase of the cross section, in agreement with the observations. The pancake orbits of case (i) have a very small m_{perp} and are probably not observed.

Frequency A could arise from the cigar-shaped Fermi surfaces about point Y, again in the sheets shown in Fig. 5(e) of

Ref. 8. This, however, does not explain the lack of angular dependence of orbit A. Sheet F also could arise from the same high energy sheet of the band structure.

In Figs. 5(c) and 5(d) of Ref. 8, close to the P point, there is a small elliptic feature of an area about three times larger than that of A. One could tentatively identify this extremal orbit with the measured frequency B. However, the angular dependence of frequency B is then not reproduced.

Frequencies C and D are degenerate for $\theta=90^\circ$. They could originate from the orbits in the xy -plane, centered at the M-point in Figs. 5(c) and 5(d) of Ref. 8. Their area is about 10% of the cross section of the Brillouin zone and not very different from the area estimated from the measured value. Again this picture does not explain the angular dependence observed for C and D. From Fig. 5(c) and 5(d) of Ref. 8, we notice that the cigar-shaped orbit centered at the Y-point (previously identified as frequency A) is nearby the orbits centered at the M-point (identified as C and D). A proximity in k -space can give rise to magnetic breakdown, resulting in a new frequency given by $D+A$. This new orbit could correspond to the observed frequency G , which could only be measured for angles close to 90° . The identification of $D+A$ as G is of course speculative, but the numerical values of the cross sections are quite close and we were not able to identify G with any other cross section in the band structure.

All of the above extremal orbits are associated with the minority spin bands. Frequency E could be tentatively identified with the lemon-like sheet of the FS as shown in Fig. 5(b) of Ref. 8 of the majority spin electrons. It should be noted that this sheet is very sensitive to even small changes in the magnetization. We do not attempt to identify frequency H .

V. SUMMARY

Angle-resolved dH-vA measurements on SrRuO₃ single crystals have resulted in the detection of at least six fundamental frequencies of oscillation. The observed frequencies range from 100 to 11 000 T and occupy between 1% and 80% of the first Brillouin zone. The effective masses for the various orbits vary from 4.1 to 6.9 m_e and the mean free path from 640 to 5500 Å or roughly 100 to 1000 times the unit cell dimensions indicating excellent sample purity. We have attempted a correspondence of the measured frequencies with the extremal orbits of the FS calculated by Santi and Jarlborg.⁸ Five of the orbits would correspond to minority spin sheets of the FS and one to majority spins. There is some agreement for the field parallel to the c -axis, however, the angular dependence of the frequencies is not reproduced satisfactorily perhaps due to limitations of the cantilever approach.

ACKNOWLEDGMENTS

The authors would like to thank D. J. Singh for useful discussions and K. Purcell and Z. X. Zhou for their assistance in data collection. This work was supported by the National High Magnetic Field Laboratory through NSF Cooperative Agreement DMR-0084173 and the State of Florida. P. S. acknowledges the support by NSF (Grant No. DMR01-05431) and DOE (Grant No. DE-FG02-98ER45707). The work done at the University of Kentucky was supported by NSF Grant No. DMR-0240831.

*Present address: Sandia National Laboratory.

†Present address: Lawrence Livermore National Laboratory.

‡Deceased.

- ¹J. J. Randall and R. Ward, *J. Am. Chem. Soc.* **81**, 2629 (1959).
- ²Y. Maeno, H. Hashimoto, K. Yoshida, S. Nishizaki, T. Fujita, J. G. Bednorz, and F. Lichtenberg, *Nature (London)* **372**, 532 (1994); K. Ishida, H. Mukuda, Y. Kitaoka, K. Asayama, Z. Q. Mao, Y. Mori, and Y. Maeno, *ibid.* **396**, 658 (1998).
- ³S. Ikeda, Y. Maeno, S. Nakatsuji, M. Kosaka, and Y. Uwatoko, *Phys. Rev. B* **62**, R6089 (2000); R. S. Perry, L. M. Galvin, S. A. Grigera, L. Capogna, A. J. Schofield, A. P. Mackenzie, M. Chiao, S. R. Julian, S. I. Ikeda, S. Nakatsuji, Y. Maeno, and C. Pfleiderer, *Phys. Rev. Lett.* **86**, 2661 (2001); S. A. Grigera, R. S. Perry, A. J. Schofield, M. Chiao, S. R. Julian, G. G. Lonzarich, S. I. Ikeda, Y. Maeno, A. J. Millis, and A. P. Mackenzie, *Science* **294**, 329 (2001).
- ⁴G. Cao, S. McCall, M. Shepard, J. E. Crow, and R. P. Guertin, *Phys. Rev. B* **56**, 321 (1997).
- ⁵D. J. Singh, *J. Appl. Phys.* **79**, 4818 (1996).
- ⁶I. I. Mazin and D. J. Singh, *Phys. Rev. B* **56**, 2556 (1997).
- ⁷P. B. Allen, H. Berger, O. Chauver, L. Forro, T. Jarlborg, A. Junod, B. Revaz, and G. Santi, *Phys. Rev. B* **53**, 4393 (1996).
- ⁸G. Santi and T. Jarlborg, *J. Phys.: Condens. Matter* **9**, 9563 (1997).
- ⁹P. Raychaudhuri, A. P. Mackenzie, J. W. Reiner, and M. R. Beasley, *Phys. Rev. B* **67**, 020411 (2003).
- ¹⁰A. P. Mackenzie, J. W. Reiner, A. W. Tyler, L. M. Galvin, S. R. Julian, M. R. Beasley, T. H. Geballe, and A. Kapitulnik, *Phys. Rev. B* **58**, R13318 (1998).
- ¹¹L. Taillefer and G. G. Lonzarich, *Phys. Rev. Lett.* **60**, 1570 (1988).
- ¹²A. P. Mackenzie, S. R. Julian, A. J. Diver, G. J. McMullan, M. P. Ray, G. G. Lonzarich, Y. Maeno, S. Nishizaki, and T. Fujita, *Phys. Rev. Lett.* **76**, 3786 (1996).
- ¹³C. S. Alexander, G. Cao, S. McCall, and J. E. Crow, *J. Appl. Phys.* **85**, 6223 (1999).
- ¹⁴L. Klein, J. R. Reiner, T. H. Geballe, M. R. Beasley, and A. Kapitulnik, *Phys. Rev. B* **61**, R7842 (2000).
- ¹⁵D. Shoenberg, *Magnetic Oscillations in Metals* (Cambridge University Press, Cambridge, 1984).
- ¹⁶L. M. Falicov and H. Stachowiak, *Phys. Rev.* **147**, 505 (1966).
- ¹⁷D. Shoenberg, *Philos. Trans. R. Soc. London, Ser. A* **255**, 85 (1963); A. B. Pippard, *Proc. R. Soc. London, Ser. A* **272**, 192 (1963).
- ¹⁸A. S. Joseph and A. C. Thorsen, *Phys. Rev.* **138**, A1159 (1965); J. H. P. Van Weeren and J. R. Anderson, *J. Phys. F: Met. Phys.* **3**, 2109 (1973).